ELSEVIER

Journal of Alloys and Compounds 408–412 (2006) 603–607

Journal of ALLOYS AND COMPOUNDS

www.elsevier.com/locate/jallcom

Study on the phase behavior of $BaEu_2Mn_2O_7$ through heat treatment of a single crystal

Naoki Kamegashira [a,*], Jian Meng [a,1], Kouji Fujita [a], Hirohisa Satoh [a],
Toetsu Shishido [b], Kazuo Nakajima [b]

[a] *Department of Materials Science, Toyohashi University of Technology,*
Tempaku-cho, Toyohashi 441-8580, Japan
[b] *Institute of Materials Research, Tohoku University, 2-1-1 Katahira, Aoba-ku, Sendai 980-8577, Japan*

Received 30 July 2004; received in revised form 30 October 2004; accepted 15 December 2004

Abstract

A new orthorhombic phase of $BaEu_2Mn_2O_7$ with the space group of *Ccmm* (no. 63) was identified for single crystals after heat treatment and its crystal structure was determined by single crystal X-ray diffractometry. The volume of the unit cell has twice the fundamental tetragonal cell and corner-shared MnO_6 octahedra are slightly distorted and Mn—O—Mn angle between the neighboring octahedra tilts with an angle by around 3° from *b*-axis. It is concluded from the results of the heat treatment of single crystals at various temperatures that this orthorhombic phase changes into a tetragonal one with superstructure ($P4_2/mnm$) at 402 K and changes once more into the fundamental tetragonal phase ($I4/mmm$) above 552 K. The tetragonal phase with superstructure which has been expected to be an unstable one is stable between the two temperatures.

Keywords: Single crystal; Crystal structure and symmetry; X-ray diffraction; Barium europium manganese oxide ($BaEu_2Mn_2O_7$)

---

1. Introduction

$BaEu_2Mn_2O_7$ is one of the layered perovskite family $BaLn_2Mn_2O_7$ (Ln = rare earth) which belong to a Ruddlesden–Popper-type homologous series $AO{\cdot}(ABO_3)_n$ with $n = 2$ [1]. A series of compounds in this family were synthesized by Deschizeaux-Cheruy and Joubert [2] changing rare earths and their results showed that these compounds fundamentally crystallize as a body centered tetragonal one with the $Sr_3Ti_2O_7$-type with the space group *I4/mmm* for Ln = Pr–Gd. Some of these also have a face-centered orthorhombic phase for Ln = Nd, Sm and Eu when these compounds were prepared in N_2 atmosphere. The body-centered orthorhombic phase are also known for Ln = Tb [3] and Gd [4]. The crystal structure of tetragonal $BaTb_2Mn_2O_7$ was refined by powder X-ray data and Rietveld analysis [5]. Although a clear boundary between two types of orthorhombic phases seems to exist between Eu and Gd, $BaGd_2Mn_2O_7$ has the two types [6] making this boundary ambiguous. Both types of orthorhombic phases exhibit phase transition into the fundamental tetragonal phase at high temperature [3,6–17]. In addition to these phases a tetragonal phase with superstructure ($P4_2/mnm$) was found in polycrystalline $BaGd_2Mn_2O_7$ [18] and single crystals of $BaGd_2Mn_2O_7$ [19] and $BaEu_2Mn_2O_7$ [20]. Furthermore compounds with more distorted monoclinic phase (*A2/m*) were for Ln = Gd [21] and Tb [17]. Therefore, many kinds of phases in this family have been known. In this paper phase behavior of $BaEu_2Mn_2O_7$ is studied using single crystals after heat treatment at various temperatures in order to clarify the relationship between these phases

---

[*] Corresponding author. Tel.: +81 532 44 6797; fax: +81 532 48 5833.
E-mail address: nkamegas@tutms.tut.ac.jp (N. Kamegashira).
[1] Present address: Key Laboratory of Rare Earth Chemistry and Physics, Changchun Institute of Applied Chemistry, Chinese Academy of Sciences, Changchun 130022, PR China.

0925-8388/$ – see front matter © 2005 Published by Elsevier B.V.
doi:10.1016/j.jallcom.2004.12.197

2. Experimental

A polycrystalline specimen of tetragonal $BaEu_2Mn_2O_7$ was prepared by the solid state reaction method from the starting materials of Eu_2O_3, $BaCO_3$ and Mn_2O_3. $BaCO_3$ and Mn_2O_3 were used after specific pretreatment to adjust stoichiometry [7,12]. Mixtures of $BaCO_3$, Ln_2O_3 and Mn_2O_3 were pressed into a pellet, heated at 1423 K for 24 h and subsequently at 1623 K for 72 h in a purified Ar atmosphere, and then slowly cooled to room temperature. Pulverization and pressing into a pellet with a rod form of these starting materials were employed to grow single crystal by floating zone (FZ) method as described in the previous paper [19,20]. After annealing these single crystals at various temperatures under Ar gas for 10 days, these specimens were slowly cooled to room temperature or rapidly quenched into ice-bath.

A suitable single crystal with size of 0.15 mm × 0.15 mm × 0.15 mm was selected and mounted on an X-ray four circle Rigaku-AFC7R diffractometer. Scanning method was 2θ-ω method and 16°/min of scan speed was used. Maximum number of scans was three Scans. Reflection data were measured with graphite-monochromated Mo Kα radiation. Intensities of three standard reflections, monitored throughout data collection, were constant within 4% of their respective mean intensities. Unit weight was given to all the observed reflections. The atomic scattering factors for neutral atoms and the dispersion correction factors were taken from International Tables for X-ray crystallography [22]. The structures were solved by direct methods using the SHELXS-97 program [23].

3. Results and discussion

As described in the previous paper [20] as-grown crystals of $BaEu_2Mn_2O_7$ having a tetragonal phase with superstructure (*P4₂/mnm*) were annealed in Ar gas at various temperatures to study phase equilibrium. When the specimen of single crystals are annealed above 673 K for 10 days and quenched to ice point, the single crystals (*P4₂/mnm*) changed into those with the fundamental tetragonal phase (*I4/mmm*) without breaking the crystal. This is because both of these tetragonal structures differ only slightly in Mn–O–Mn tilt angles connecting octahedra composing the skeleton of the layered perovskite, where the oxygen octahedral regularly line up in the fundamental tetragonal phase with *I4/mmm* space group, while superlattice caused by mutual tilting of octahedral is characteristic of the other tetragonal phase with *P4₂/mnm* space group. The relationship between these two tetragonal phases is $a_s \approx \sqrt{2}a$, where a_s and a are the lattice constants of *P4₂/mnm* and *I4/mmm*, respectively. These results are in good agreement with the previous data in which the phase transition of $BaEu_2Mn_2O_7$ exists near 550 K [23–23]. But a new phase appeared when the specimen of single crystals (*P4₂/mnm*) were annealed at 453 K for 10 days and very slowly cooled to room temperature. Dur-

Table 1
Experimental conditions and crystal data of $BaEu_2Mn_2O_7$ with *Ccmm* space group

Crystal (453 K slow cool)	
Crystal system	Orthorhombic
Space group	*Ccmm*(63)
a (nm)	0.5538(2)
b (nm)	2.0132(3)
c (nm)	0.5538(3)
V (nm^3)	0.6174
Z	4
D (g cm^{-3})	7.1338
Crystal size (mm^3)	0.15 × 0.15 × 0.15
Color	Black
Experiment method	
Diffractometer	Rigaku AFC7R
λ (Mo Kα) (Å)	0.71069
2θ (°)	120
No. of observation ($I > 4\sigma(I)$)	616
Refinement	
Thermal parameter	Anisotropic
R_1:wR_2:S	0.0719:0.1687:1.212

$$R_1 = \frac{\sum ||F_0|-|F_c||}{\sum |F_0|} \text{ and } wR_2 = \left\{ \frac{\sum [w(F_0^2-F_c^2)^2]}{\sum [w(F_0^2)^2]} \right\}^{1/2}.$$

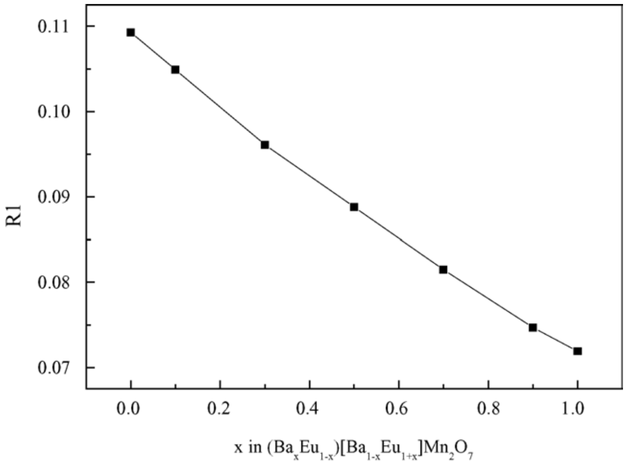

Fig. 1. Variation of R1-factor with x, degree of distribution of Ba and Eu atoms in A-site (4c and 8g) of $(Ba_xEu_{1-x})[Ba_{1-x}Eu_{1+x}]Mn_2Mn_2O_7$ with *Ccmm* space group, where parenthesis and bracket show 4c and 8g sites, respectively.

Table 2
Atomic parameters of $BaEu_2Mn_2O_7$ with *Ccmm* space group

Atom	Site	*x/a*	*y/b*	*z/c*
Ba	4c	0.2557(1)	0.5000(9)	0.7500
Eu	8g	0.2689(1)	0.68349(3)	0.7500
Mn	8g	0.7536(2)	0.6024(1)	0.7500
O1	4c	0.770(3)	0.5000(2)	0.7500
O2	8g	0.699(2)	0.7088(7)	0.7500
O3	8e	0.0000	0.3839(6)	0.0000
O4	8e	0.5000	0.6042(5)	0.0000

Table 3
Anisotropic displacement parameters of $BaEu_2Mn_2O_7$ with *Ccmm* space group

Atom	Site	U11	U22	U33	U23	U13	U12
Ba	4c	0.0104(3)	0.0126(5)	0.0115(5)	0.0000	0.0000	0.0000
Eu	8g	0.0120(3)	0.0111(4)	0.0230(4)	0.0000	0.0000	0.0000(1)
Mn	8g	0.0086(5)	0.0134(8)	0.0111(8)	0.0000	0.0000	0.0002(3)
O1	4c	0.032(9)	0.03(1)	0.037(9)	0.0000	0.0000	0.0000
O2	8g	0.019(5)	0.034(7)	0.12(1)	0.0000	0.0000	0.003(4)
O3	8e	0.008(2)	0.046(5)	0.015(3)	0.0000	−0.000(2)	0.0000
O4	8e	0.013(3)	0.030(4)	0.018(3)	0.0000	−0.004(3)	0.0000

ing these phase transition single crystals were not broken and a state of single crystals was kept, judging from the non-broken Bragg peaks measured by four circle diffractometer. The space group of this new orthorhombic phase was determined to be *Ccmm* as follows: the symmetry of intensities of $BaEu_2Mn_2O_7$ revealed orthorhombic one with the lattice constants $a = 0.5538(2)$ and $b = 2.0132(3)$ and $c = 0.5538(3)$ nm. The conditions of systematic absences of X-ray peaks for each sample revealed. The possible space groups compatible were *Ccmm* (no. 63), *Ccm21* (no. 36) and *Cc2m* (no. 40). Among these space groups *Ccm21* and *Cc2m* are not centrosymmetric and have polarity and low electrical conductivity such as ferroelectric substances, while only Ccmm is centrosymmetric. As our previous experimental results show that $BaEu_2Mn_2O_7$ have considerably high electrical conductivity [12] and so no possibility of ferroelectricity could be expected. Therefore, this compound should be centrosymmetric and *Ccmm* was chosen as the space group for an orthorhombic $BaEu_2Mn_2O_7$. Although the lattice parameters *a* and *c* are almost the same, any possibilities of tetragonal symmetry was excluded from the magnitude of the reliability factor derived by the crystal structure analysis. For example, the analysis assumed by the *$P4_2/mnm$* space group resulted in 0.35 for R1-factor and this space group could be excluded. The crystal data and experimental condition of the $BaEu_2Mn_2O_7$ sample annealed under the above conditions are shown in Table 1. Maximum and minimum values of measured reflections were $0 \leq h \leq 10$, $0 \leq k \leq 31$ and $0 \leq l \leq 8$. Several models for occupation for Ba and Eu ions in the A-site were attempted and the results are shown in Fig. 1 where the ordering model of all the Ba ions in 4c and all the Eu ions in 8g results in the singly occupied one.

Table 4
Selected bond length and angles of $BaEu_2Mn_2O_7$ with *Ccmm* space group

Bond length (nm)		Angle (°)	
Eu–O2	0.220(1)	Mn–O1–Mn	174.8(9)
Eu–O2	0.243(1)	Mn–O3–Mn	163.8(7)
Eu–O2	0.2821(3) × 2	Mn–O4–Mn	177.9(6)
Eu–O2	0.320(1)	O1–Mn–O2	174.5(6)
Eu–O4	0.2471(6) × 2	O1–Mn–O3	96.3(5)
Ba–O1	0.2773(2) × 2	O1–Mn–O4	92.9(4)
Ba–O1	0.285(2)	O2–Mn–O3	87.6(4)
Ba–O3	0.3064(9) × 4	O2–Mn–O4	83.2(4)
Ba–O4	0.2854(7) × 4	O3–Mn–O3	89.7(1)
Mn–O1	0.2063(2)	O3–Mn–O4	89.85(6)
Mn–O2	0.216(1)		170.8(5)
Mn–O3	0.1963(2) × 2		
Mn–O4	0.1973(1) × 2		

The final positional parameters and thermal parameters are shown in Tables 2 and 3, respectively. The interatomic distances and angles are given in Table 4 together with their estimated standard deviation.

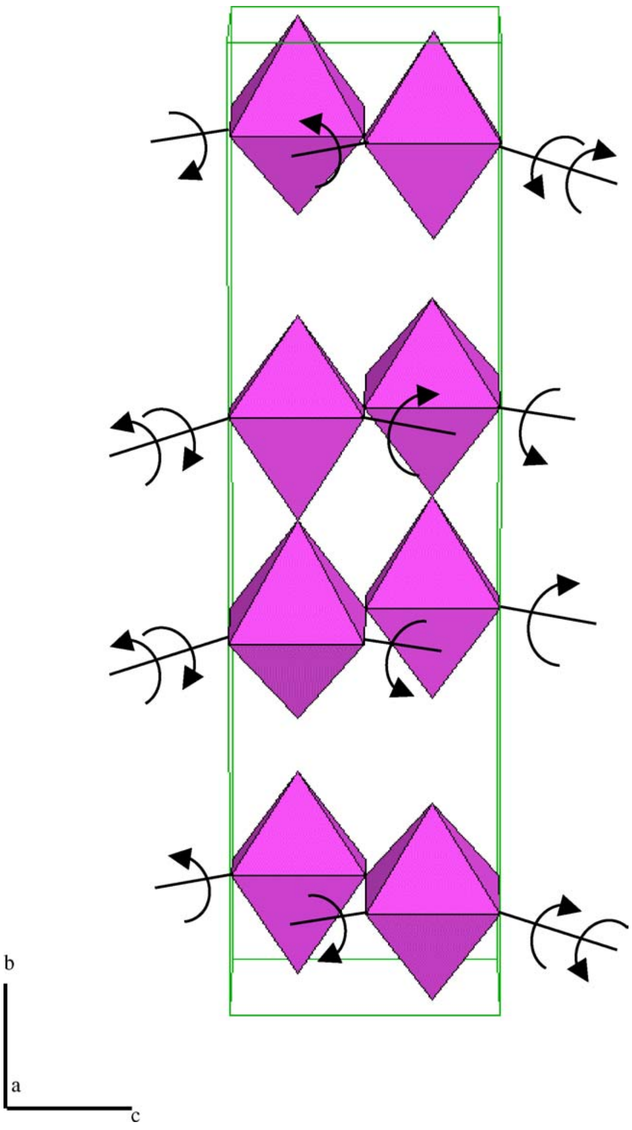

Fig. 2. Overview of crystal structure of $BaEu_2Mn_2O_7$ with *Ccmm* space group with an emphasis on tiltin mode of oxygen octahedron.

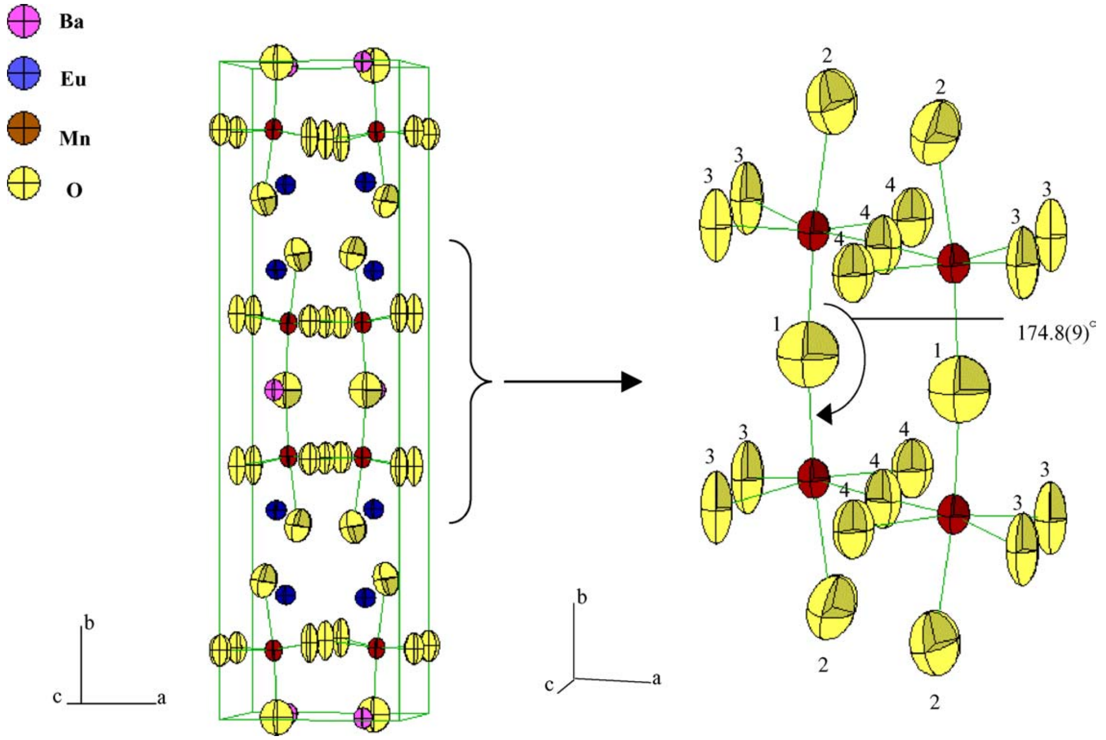

Fig. 3. Thermal vibration of $BaEu_2Mn_2O_7$ with *Ccmm* space group.

The MnO_6 octahedron is distorted as shown in Fig. 2. Four oxygen ions, two O3 and two O4 ions, coordinate to a central Mn ion on the plane almost perpendicular to the *b*-axis with a shorter distances (mean distance = 0.197 nm). This mean distance is a little shorter than the sum of the ionic radii of O^{2-} and Mn^{3+} ions (0.205 nm) [24]. While Mn–O1 distance is longer a little which is nearly equal to the theoretical value and only Mn–O2 distance is much longer. One of the reasons is because O2 ions are located on the outer end of perovskite blocks in this structure. There is also another possibility of Jahn–Teller effect for the reason of the distortion because trivalent Mn ion is included in this compound. The schematic view of the rotation of the octahedra in double block layer caused by a slight tilt is shown in Fig. 3. The crystal structure is shown in Fig. 4.

The anisotropic thermal vibration ellipsoids are shown in Fig. 4 and it is derived from this figure that an overall vibration elongates along *b*-axis, which is the longitudinal direction of the layered perovskite. A characteristic feature of the anisotropic thermal vibration is seen for O2, an end ion of each octahedron.

Thermal analysis was carried out using the pulverized sample of single crystals with *P4₂/mnm* space group. This powder was annealed at 453 K in Ar for 10 days and slowly cooled to room temperature which is the same treatment as single crystals for a formation of a new orthorhombic phase with *Ccmm* space group. The result of DSC measurement is shown in Fig. 4 and four thermal anomalies are observed at 367, 402, 519 and 552 K. After single crystals with *Ccmm* prepared as above were annealed at several temperatures between these four peaks and also at several temperatures below 367 K and above 552 K for 10 days in Ar and then quenched to room temperature, the crystal structure of each phase was again refined by four circle single crystal X-ray analysis. It was identified that *Ccmm* phase is stable below 402 K, *P4₂/mnm* phase is stable between 402 and 552 K and *I4/mmm* phase is stable above 552 K. The reason for the other two peaks in DSC curve at 367 and 519 K are not characterized. The derived phase diagram for transition temperature and oxygen non-stoichiometry is schematically shown in Fig. 5, taking into consideration of our previous results that

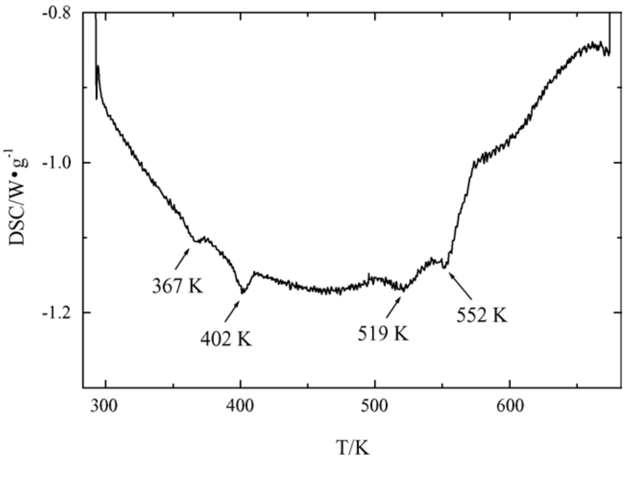

Fig. 4. DSC diagram for the sample of $BaEu_2Mn_2O_7$ with *Ccmm* space group.

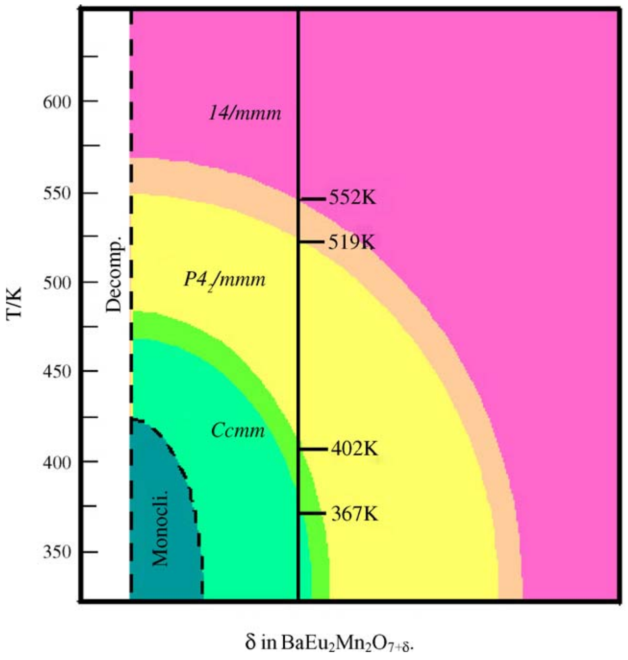

Fig. 5. Schematic phase diagram of temperature against oxygen non-stoichiometry for $BaEu_2Mn_2O_{7+\delta}$.

the transition temperature decreases with increase of oxygen non-stoichiometry (δ) [12,14].

Acknowledgement

This work was supported by the Grant-in-Aid for Scientific Research (B) (No. 13450259) by the Japan Society for the Promotion of Science.

References

[1] S.N. Ruddlesden, P. Popper, Acta Crystallogr. 11 (1958) 54–55.
[2] M.N. Deschizeaux-Cheruy, J.C. Joubert, J. Solid State Chem. 40 (1981) 14–19.
[3] N. Kamegashira, S. Umeno, Mater. Chem. Phys. 16 (1986) 89–98.
[4] N. Kamegashira, A. Shimono, M. Horikawa, Mater. Chem. Phys. 24 (1990) 389–397.
[5] J. Meng, H. Satoh, N. Kamegashira, J. Alloys Compd. 244 (1996) 75–78.
[6] N. Kamegashira, H. Satoh, M. Horikawa, Mater. Lett. 10 (1991) 494–496.
[7] N. Kamegashira, S. Umeno, Jpn. J. Appl. Phys. 25 (1986) L238–L239.
[8] N. Kamegashira, S. Umeno, Mater. Lett. 4 (1986) 236–238.
[9] N. Kamegashira, M. Icikawa, S. Umeno, M. Aoki, Mater. Chem. Phys. 17 (1987) 585–590.
[10] N. Kamegashira, S. Umeno, H. Satoh, M. Horikawa, Mater. Chem. Phys. 24 (1989) 83–88.
[11] A. Shimono, N. Kamegashira, Mater. Chem. Phys. 21 (1989) 307–311.
[12] N. Kamegashira, M. Ichikawa, Mater. Chem. Phys. 25 (1990) 71–79.
[13] A. Shimono, K. Hayashi, N. Kamegashira, Mater. Chem. Phys. 28 (1991) 175–190.
[14] H. Satoh, M. Horikawa, N. Kamegashira, J. Alloys Compd. 192 (1993) 99–101.
[15] H. Satoh, M. Horikawa, N. Kamegashira, Netsu Sokutei 20 (1993) 193–197.
[16] J. Meng, J. Wang, J. Peng, H. Satoh, N. Kamegashira, in: S.H. Feng, J.S. Chen (Eds.), Frontiers of Solid State Chemistry, World Scientific, 2002, pp. 159–165.
[17] N. Kamegashira, J. Meng, T. Mikami, H. Satoh, N. Kakuta, K. Fujita, J. Rare Earths 22 (2003) 17–21.
[18] N. Kamegashira, H. Satoh, T. Mikami, J. Alloys Compd. 311 (2000) 69–73.
[19] N. Kamegashira, J. Meng, T. Mori, A. Murase, H. Satoh, T. Shishido, T. Fukuda, Mater. Lett. 57 (2003) 1941–1944.
[20] N. Kamegashira, J. Meng, T. Murase, K. Fujita, H. Satoh, T. Shishido, T. Fukuda, 10th International Ceramics Congress Part A (Ed. P. Vincenzini, Techna Srl) (2003) 181–186.
[21] J. Meng, A. Murase, H. Satoh, N. Kamegashira, Proceedings of the Fourth International Conference on Rare Earth Development and Application, China, 2001, pp. 183–186.
[22] T. Hahn, International Tables of Crystallography, vol. A, Kluwer, Boston, 1992.
[23] G.M. Sheldrick, SHELXS-97: The SHEX-97 Manual, University of Göttingen, Germany, 1990.
[24] R.D. Shannon, C.T. Prewitt, Acta Crystallogr. B25 (1969) 925–946.